Egypt. J. Phys. **Vol. 50,** pp. 1-11 (2022)

Egyptian Journal of Physics
http://ejfs.journals.ekb.eg/

Effect of Sb_2O_4 on Structural, Physical and Optical Properties of Sodium Zinc Borate Glasses

A. H. Ghanem[1*] , A. H. Serag El-Deen[2] and Azza El-Sayed[1]
[1]Physics Department, Faculty of Science, Fayoum University, Fayoum, Egypt.
[2]Physics Department, Modern Academy for Engineering and Technology, Egypt.

ANTIMONY doped sodium zinc borate glasses of composition [(65-x) B_2O_3-10ZnO-25Na_2O-xSb_2O_4] (where x = 0, 5, 10, 15 and 20 in mol%) were prepared by using the conventional melt quenching technique. The characterization of the samples was done by X-ray diffraction. XRD pattern revealed the amorphous nature of the prepared samples. Various physical and optical parameters such as density, molar volume, oxygen molar volume, oxygen packing density, optical bandgap energy and Urbach energy were evaluated. The opposite trend between density and molar volume as well as the opposite behaviour between oxygen molar volume and oxygen backing density revealed that the glass samples become less open. FTIR spectra have been investigated at room temperature and used to estimate N_4 ratio and its dependent on composition. FTIR analysis showed that antimony oxide acts as a modifier in the borate glass doped with ZnO and Na_2O. The observed data clearly suggests that the investigated glass samples may be used for optical limiting applications.

Keywords: Optical properties; Borate glass; Sb_2O_4 antimony oxide; Energy gap; FTIR; N_4 ratio.

Introduction

Glassy materials exhibit an important and fundamental role in science and modern technology. Borate glass is one type of glasses which find a wide range of applications. In borate glasses, boron oxide is the fundamental glass former which is characterised by its higher field strength, lower cation size and small heat of fusion. In borate glasses, boron atoms are triangularly coordinated with either three or four oxygen atoms forming trigonal BO_3 or tetrahedral BO_4 structural units. These two bases units of the borate glass can arbitrarily be combined to form either superstructural units or different B_xO_y groups like boroxol ring, pentaborate, tetraborate and diborate groups,…. etc. The fraction of these structural units depends on the structure and concentration of the added modifiers [1-5].

Antimony oxides, Sb_xO_y, have been known as glass formers [6]. According to stoichiometries, antimony is known to form three binary oxides of the form Sb_2O_x, where x = 3, 4, 5. Antimony trioxide Sb_2O_3 (Sb^{III}), antimony tetroxide Sb_2O_4, and antimony pentoxide Sb_2O_5 (Sb^{v}) are three types of antimony oxides. Antimony trioxide is a common oxide used as a former in many borate glasses. It takes two crystalline forms:- a-Sb_2O_3 (senarmontite) and b-Sb_2O_3 (valentinite). Senarmontite is the stable phase under circumstant condition, while valentinite is observed at high temperature and pressure. In the senarmontite structure, covalently bonded Sb_4O_6 units are closely packed in a face centred cubic. The building blocks of these units are the pyramidal SbO_3. Valentinite form takes the same structure as senarmontite form. Antimony tetroxide (Sb_2O_4) exhibits the structural features of antimony tri and pent oxide. Antimony tetroxide is a mixed valency compound containing both Sb^{3+} and Sb^{5+} ions in equal proportions in its crystal lattice. It is stable around 1000°C [7, 8].

Antimony oxide glasses was predicted by Zachariasen [6] and confirmed by various authors [9, 10]. Antimony containing glasses have received considerable interest because of their significant scientific and practical applications in the field of optics and electronics as in the case of many heavy metals such as Zn, Bi, Pb, Ba,...etc [9, 11-15].

*Corresponding author:ahm04@fayoum.edu.eg
DOI :10.21608/ejphysics.2021.49672.1059
Received : 6/12/2020; accepted : 21/1/2021

To our knowledge, the most recent antimony glass publications focus on Sb_2O_3 antimony trioxide based glass. No structural work on ZnO-Na_2O-B_2O_3-based glasses containing Sb_2O_4 oxide has been reported in the literature. Our goal of this study is therefore to investigate the effect of the addition of Sb_2O_4 on the structural, physical and optical properties of sodium zinc borate glasses.

Experimental Procedures

Samples preparation

Borate glasses doped with Sb_2O_4 of the composition (65-x)% B_2O_3-10% ZnO-25%Na_2O-x%Sb_2O_4 (where x =0, 5, 10, 15, 20 mol%) were prepared by using traditional method of melt quenching. In powder form, the starting materials were used, namely boric acid (H_3BO_3), zinc oxide (ZnO), sodium carbonate (Na_2CO_3), and antimony oxide (Sb_2O_4). The mixed powders were melted in ceramic crucibles at 1000°C for one hour, then the melt was shaken every 20 min to achieve homogenous melting. The melt was poured into preheated copper rectangular moulds. The glasses were annealed at 300°C for four hours to remove the internal stresses from the glass samples before leaving it to cool down slowly to room temperature.

Measurements

X-ray measurements are performed on a fully computerized X-ray diffractometer, Shimadzu XRD-6000. XRD patterns in the range $4^o < 2\theta < 90°$ were obtained at a scan rate of 2°/ min using CuKα1 radiation source, a generator voltage of 40 kV and a current of 40 mA.

Archimedes method [16] was used to determine the density of the glass samples at room temperature using 4- digit microbalance (AnD, HR200) with toluene as an immersion fluid with the help of the following formula:-

$$\rho = W_a/(W_a - W_b) \times \rho_b \quad \ldots\ldots(1)$$

where and are the weight of the glass samples in air and in the toluene fluid respectively, is the toluene density and is equal to 0.87g/cm^3. The corresponding molar volume V_m for studying the physical properties of the glass samples were calculated using the relation [17-20].

$$V_m = M_T/\rho \quad \ldots\ldots(2)$$

where M_T is the total molecular weight of the mixture.

The structural parameters, oxygen molar volume (V_0) and oxygen packing density (OPD), have been determined with the values of density r and molar volume V_m using the following equations [21, 22, 23]:

$$V_0 = V_m/(\sum_i x_i n_i) \quad \ldots\ldots(3)$$

where x_i is the molar fraction of each component i and n_i is the number of an oxygen atom in each constituent oxide. Oxygen packing density (OPD) was determined by the following equation:

$$OPD = 1000 \times C(\rho/M) \quad \ldots\ldots(4)$$

where C is the number of oxygen atoms per each composition and M is the molecular weight of the glass sample.

The optical absorption spectra of the prepared glass samples were recorded at room temperature using UV-visible spectrophotometer model (JASCO V-670 UV/VIS) in the wavelength range from 200 nm to 1100 nm.

KBr pellet technique at room temperature in the wavenumber range 400-4000 cm^{-1} was used to obtain the infrared spectra of the present glass samples. The spectra were recorded by Fourier transform computerized spectrometer type (Thermo Nicolet 200 spectrometer).

Results and Discussions

XRD patterns, of the prepared glass samples listed in Table 1, are shown in Fig. 1. It reveals a characteristic of the non-crystalline nature of the prepared glass samples. This is most likely due to the absence of long-range order, indicating the glassy nature of the samples.

The key parameters for exhibiting physical and structural properties, such as compactness or softness, cross-linking and coordination number....etc, of the prepared glass samples, are density (ρ), molar volume (V_m), oxygen molar volume (V_o) and oxygen packing density (OPD). The values of these parameters are listed in Table2.

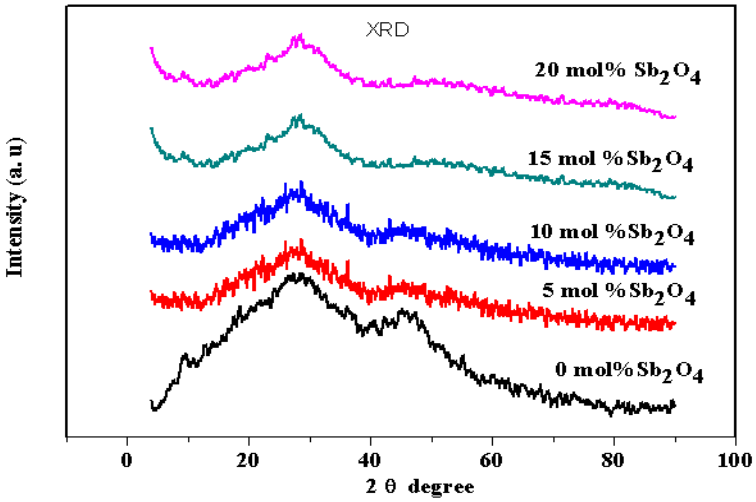

Fig. 1. X-ray diffraction patterns of (65-x) B_2O_3-10ZnO-25Na_2O-xSb_2O_4 glasses.

TABLE 1. Nominal composition (in mol %), of the prepared glass samples.

Samples	Composition (mol %)			
0	65 B_2O_3	0Sb_2O_4	10ZnO	25Na_2O
5	60 B_2O_3	5Sb_2O_4	10ZnO	25Na_2O
10	55 B_2O_3	10Sb_2O_4	10ZnO	25Na_2O
15	50 B_2O_3	15Sb_2O_4	10ZnO	25Na_2O
20	45 B_2O_3	20Sb_2O_4	10ZnO	25Na_2O

TABLE 2. Density (r), molar volume (V_m), oxygen molar volume (V_0) and oxygen backing density (OPD) of the glass samples.

Samples	Density r (g/ cm^3)	Molar volume Vm (cm^3/ mol)	Oxygen molar volume Vo (cm^3/mol)	Oxygen packing density OPD (mol/L)
0	2.5	46.05	20.02	49.95
5	2.77	44.78	19.06	52.48
10	3.06	43.53	18.14	55.13
15	3.29	43.24	17.65	56.66
20	3.50	43.27	17.31	57.78

Table 2 shows that an increment and decrement in the values of the density and of the molar volume with the increase of Sb_2O_4 concentration. The increment in density is due to the substitution of the lower B_2O_3 molecular weight (123.6 g/ mol) with the higher Sb_2O_4 molecular weight (289.99 g/mol.). While the decrement in the molar volume may be due to the difference in the volume of molecules between B_2O_3 and Sb_2O_4. The increment in the density and the decrement in the molar volume with the addition of Sb_2O_4 indicate the glass becomes less open [24]. A small reduction in oxygen molar volume and the increase in oxygen packing density confirm that the glass becomes less open. This indicates that the rate of producing the non-bridging oxygen decreases with antimony content.

The structure of the glass samples was analyzed by the optical absorption spectra at room temperature using the UV spectrometer. The UV-visible spectra of the glass samples are shown in Fig. 2. It is seen that the glass samples prepared are optically transparent. For all wavelengths longer

than 400 nm, it exhibits a strong transparency window. The absorption edge is not sharply defined and extends over a wide wavelength range of 1200 nm, as shown in Fig.2. This is consistent with verifying the glass character of the glass samples studied in conjunction with the findings of the XRD. Also, it shows that the edge of UV absorption spectra shifted with increasing Sb_2O_4 concentration towards the longer wavelength, i.e. red shift.

To study the optical properties of the glass samples, it must determine the mechanism of optical absorption and optical bandgap by using the equation [25, 26].

$$\alpha(v)= (B[(hv-E_g)]^n)/hv \quad \ldots\ldots(5)$$

where α(n) is the absorption coefficient as a function of photon energy, B is constant and is the optical bandgap. In amorphous systems, for direct transition n = 1/2 and indirect transition n = 2. The optical bandgap for the direct and indirect transition was estimated from the plot of $(\alpha hn)^2$ and $(\alpha hn)^{1/2}$ as a function of photon energy hn. It is calculated by extrapolating the linear portion of the plot to reach $(\alpha hn)^2 = 0$ and $(\alpha hn)^{1/2}=0$. In the non-crystalline system, the indirect transition is the most probable absorption mechanism due to the absence of translation symmetry. Optical bandgap data for the indirect transition of the present system (65-x)% B_2O_3-10% ZnO-25%Na_2O-xSb_2O_4 mol% is shown in Fig. 3.

Band tail width of the localized states (Urbach energy) can be calculated using the empirical relation [27]:

$$\alpha(\searrow)=\alpha_{(0)}\, e^{(hv/\Delta E)} \quad \ldots\ldots(6)$$

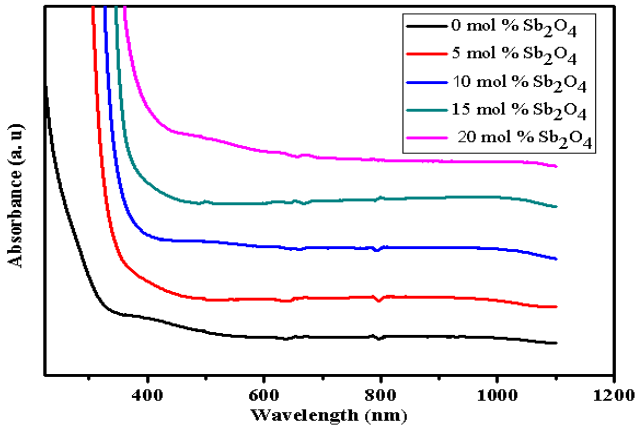

Fig. 2. Optical absorption spectra of the prepared glass samples with different Sb_2O_4 concentrations.

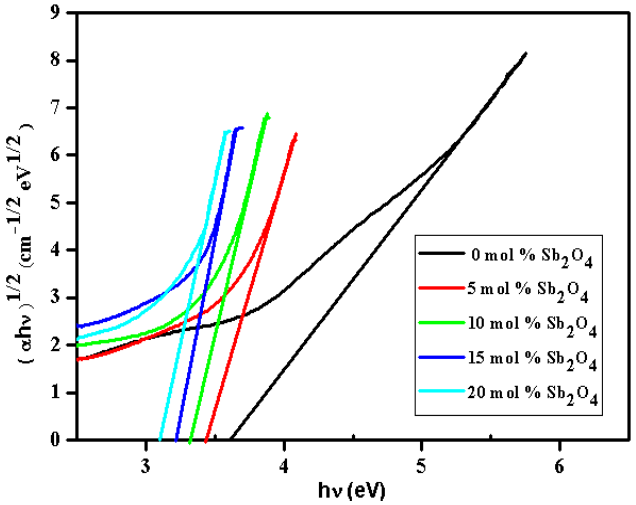

Fig. 3. Plots of $(\alpha hn)^{1/2}$ versus (hn) of the prepared glass samples with different Sb_2O_4 concentrations.

where α_0 is a constant, DE is the Urbach energy (E_u) which indicates the width of the band tails of the localized states and n is the frequency of the radiation.

Urbach energy (E_u) obtained from reciprocal of the graph slope of logarithm of absorption coefficient (lnα) versus the photon energy (hn) [16, 26, 28]. Such a plot is shown in Fig. 4. The deduced values of the optical bandgap and Urbach energy versus Sb_2O_4 concentrations are shown in Fig. 5. It is observed that the optical band gap of indirect transitions follows the opposite trend to the Urbach energy. The optical bandgap decreases while Urbach energy increases. This behaviour exhibiting structural changes in the glass network. This is attributed to the increase of Sb_2O_4 content increases both boron tetrahedral units BO_4 and bridging oxygen. Due to the increase in Sb_2O_4 concentrations, Sb^{+3} and Sb^{+5} ions increases [29, 30] and due to the melting process Sb^{+3} transfer to Sb^{+5} [31]. Therefore, the configurations of Sb_2O_4 mainly consist of SbO_5 octahedral geometry. Hence, Sb^{+5} ions introduce into the glass as singly positive SbO_4. This is due to breaking Sb-O bonds of SbO_5 and therefore, producing boron tetrahedral BO_4 units and bridging oxygen [32, 33]. This results in a decrease in the optical band gap and shifts the UV-visible absorption spectral edge towards a high wavelength. This behaviour exhibits good agreement with obtained IR spectra.

Infrared absorption spectra for the investigated glass samples are shown in Fig.6. It shows that the band at 806 cm^{-1} which is assigned to the boroxol ring in the borate glass network does not found in the present glass samples. This indicates the absence of a boroxol ring and hence the glass system contains BO_3 and BO_4 groups [34,35]. This is may be due to antimony oxide disrupted the boroxol rings in the alkali borate glass structure. This conclusion was confirmed with that reported by Terashima et al. for binary antimony borate glasses [32].

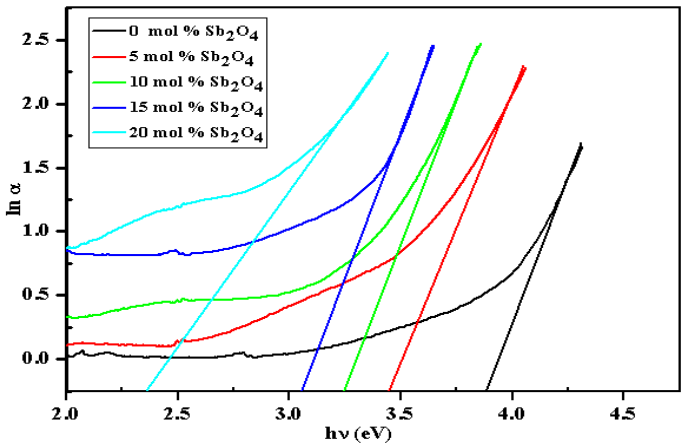

Fig. 4. Plots of lna versus hn of (65-x) B_2O_3-10ZnO-25Na_2O-xSb_2O_4 glass system.

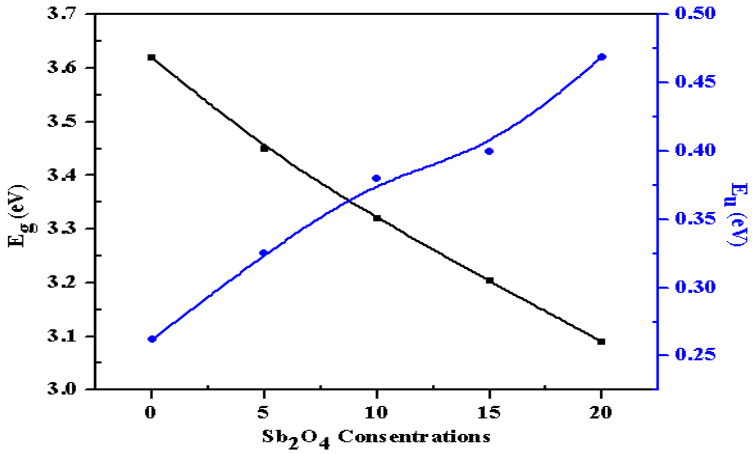

Fig. 5. Optical band gap and Urbach energy versus Sb_2O_4 concentrations.

Figure 6 shows also that the IR spectrum of the present glass (65)% B_2O_3-10% ZnO-25%Na_2O-0%Sb_2O_4, was composed of mainly four vibrational bands located at 600-800, 800-1200, 1200-1600 and at 3250-3750 cm^{-1}. In this respect, a deconvolution of IR spectra for all Sb_2O_4 concentrations, to determine the ratio N_4, and their assignments are shown in Table 3 and Fig. 7.

The broadband appears within the ranges 800-1200 and 1200-1600 cm^{-1} is composed of several individual peaks at 939, 1089 cm^{-1} and 1228, 1353, 1506 cm^{-1}, respectively. These peaks are ascribed to the B-O stretching vibrations of BO_4 tetrahedral units and BO_3 trigonal units, respectively, as listed in Table 3 [36, 37]. While the small bands that appear in the ranges 600-800 and 3250-3750 cm^{-1} are composed of individual peaks at 611, 701 cm^{-1} and 3500 cm^{-1} respectively. These peaks are due to B-O-B bending vibration of BO_3 groups and due to B-OH or water groups respectively [36-38]. The presence of B-OH groups ascribe to the KBr technique and also arise from the water in H_3BO_3. As Sb_2O_4 concentration increases from x=5 mol% to x= 20 mol%, the intensity of these bands in the whole regions increases and their peak positions change as well as the appearance of a new band around 500 cm^{-1}. Peaks in the region 600-800 cm^{-1} are shifted toward higher wavenumbers 625, 716 cm^{-1}, while that in the regions 800-1200 and 1200-1600 cm^{-1} are shifted to lower wavenumbers 903, 1056 cm^{-1} and 1214, 1327, 1473 cm^{-1}, respectively.

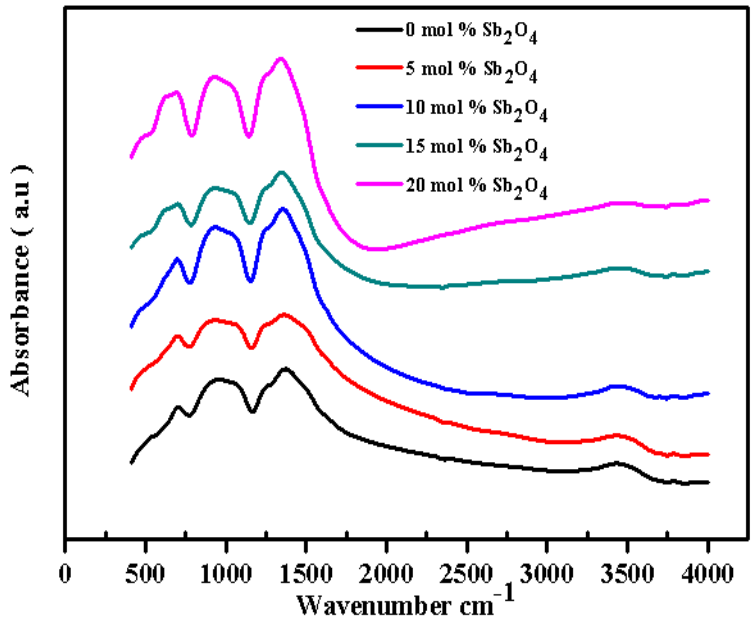

Fig. 6. FTIR spectra of all investigated glass samples.

TABLE 3. Assignments of absorption bands of the infrared spectra of the prepared glass samples.

Wavenumber (cm^{-1})	Assignment
600-800	Bending vibration of Sb-O-B in BO_3 trigonal units.
800-1200	Stretching vibration of B-O bonds in BO_4.
1200-1600	stretching vibrations of B-O of trigonal BO_3 units.
2500-4000	Hydrogen bonding of molecular water.

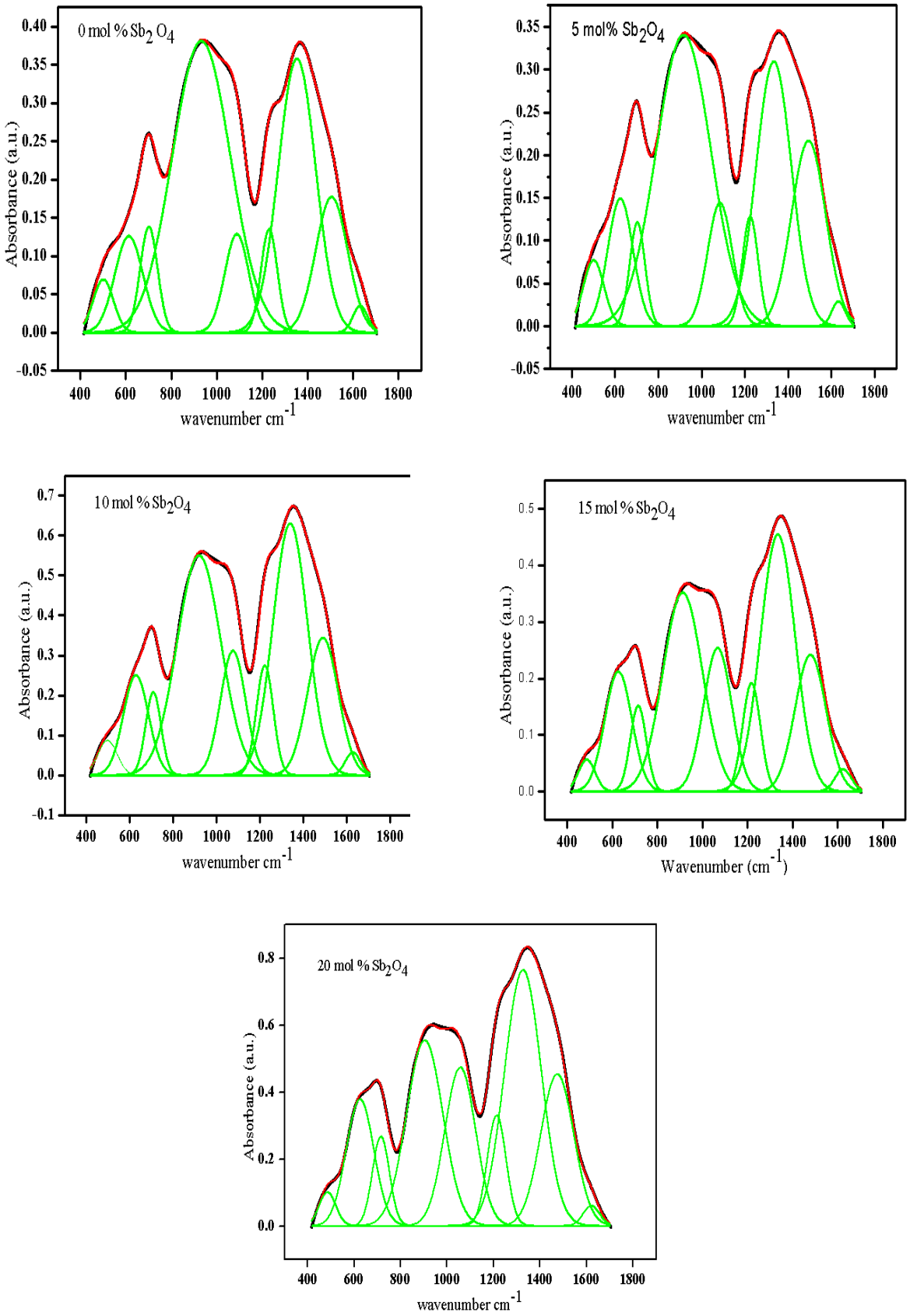

Fig. 7. Deconvolution of FTIR spectra of the glass samples.

According to the concept of Tarte and Condrate [39, 40] and applied by Dimitriev et al. [41] in the interpretation of the observed FTIR spectra with the aid of the deconvoluted spectra shown in Fig. 7, the increase in the intensity in the region 800-1200 cm^{-1} and their shifting beaks toward the lower wavenumber when B_2O_3 concentration decreases are due to the increase in the stretching vibration of BO_4 tetrahedral units. This is ascribed to breaking Sb-O bonds of SbO_5 units with the addition of Sb_2O_4 to form 4-coordinated units (SbO_4) and provide a charge balance for the negative $(BO_4)^-$ and producing the bridging oxygen [32,42,43]. This gives the conclusion that Sb^{5+} ions play an important role in charge compensator in the present glass samples as that predicted by Gangareddy et al. [35] in Sb_2O_3-B_2O_3 glass system. Whereas the increase in the intensity in the region 1200-1600 cm^{-1} and shifting their beaks towards lower wavenumbers is attributed to the increment of stretching vibration of BO_3 structure units and non-bridging oxygen [44]. This is may be due to the bending vibration of pyramidal SbO_3 since Sb_2O_4 consists of two equal amount of Sb^{+3} and Sb^{+5} ions [29]. Also, the increase in the intensity of the band in the region 600-800 cm^{-1} is attributed to the bending vibration of BO_3 [36-38]. This may be due to the formation of asymmetric vibration of B–O–Sb bonds formed by merging of Sb–O–Sb bridges with B–O–B linkages [45, 46]. This means that the number of Sb-O-B bonds increases with the decrease in the number of Sb–O–Sb and B-O-B bonds. Thus the addition of Sb_2O_4 to the present glass samples gives extra oxygen atoms to build up of SbO_4 and BO_4 tetrahedral units [47, 48, 49]. Furthermore, the appearance of a new band at 500 cm^{-1} with the increase in Sb_2O_4 content ascribed to the bending vibrations of SbO_3 pyramids [50]. The formation of this band deduces that an increase in the concentration of BO_3 units and non-bridging oxygen [51]. Therefore, the addition of Sb_2O_4 to ZnO-Na_2O-B_2O_3 glasses changing the structural configuration of the studied glass samples by enhancement the rate of producing BO_3 trigonal units than tetrahedral BO_4 units with producing non-bridging oxygen. Therefore, Sb_2O_4 can be considered as a modifier. Thus the creation of non-bridging oxygen due to the incorporation of Sb_2O_4 in the glass samples enhancement the nonlinear optical properties (NLO) [52, 53]. This result is confirmed with the decrease in N_4 ratio. N_4 is defined as [50, 51]:

(concentration of BO_4)/(concentration of (BO_4+BO_3))……(7)

The calculated values of the N_4 ratio are shown in Fig. 8. It shows a common decrease in N_4 ratio as Sb_2O_4 concentration increases. This may be attributed to the rate of increase of BO_4 units are small concerning the symmetric vibration of BO_3 units. The decrement in N_4 ratio in Sb_2O_4–B_2O_3-ZnO-Na_2O glasses indicates the glass becomes less open and reflects the ability of Sb_2O_4 to act as modifier oxide in the borate network [32]. This result agrees with density (r), molar volume (V_m), oxygen molar volume (V_o), oxygen backing density (OPD) and energy gap (E_g) calculations.

From the above argument, FTIR spectra reveal clearly that the addition of antimony oxide to Na_2O-ZnO-B_2O_3 glasses plays an important role in charge compensator for $(BO_4)^-$ and the creation of the non-bridging oxygen and to act as a modifier. Hence, with the addition of Sb_2O_4, the structure and the properties of the prepared glass alters [35]. Therefore, it enhancement the nonlinear optical properties (NLO).

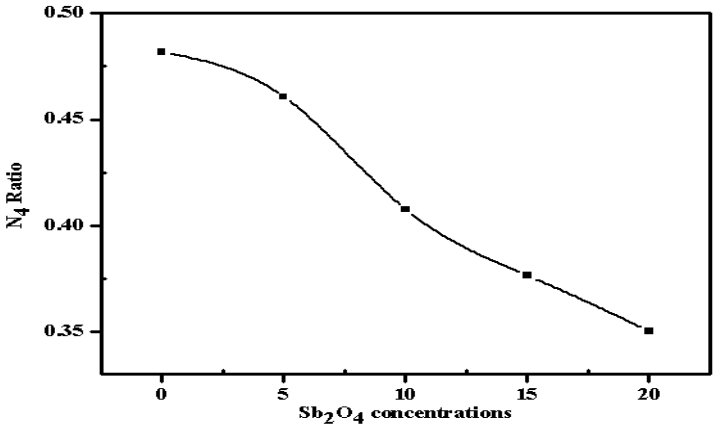

Fig. 8. N_4 ratio versus Sb_2O_4 concentrations.

Conclusion

Physical, optical properties and the structure of the glassy system of the form (65-x)% B_2O_3-10%ZnO-25%Na_2O-x%Sb_2O_4 (where x =0, 5, 10, 15, 20mol%) have been carried out by density, molar volume, oxygen molar volume, oxygen backing density, x-ray diffraction, UV optical absorption spectra and Fourier transformation infrared spectroscopy (FTIR). X-ray diffraction was revealed the non-crystalline nature of the prepared glass samples. The optical band gap (E_g) and Urbach energy (E_u) were evaluated using optical UV-Visible spectral measurements. Optical absorption spectra revealed that the decrease in bandgap energy with the increase of antimony concentration attributed to the increase of boron tetrahedral units BO_4. FTIR analysis shows that the dependence of the number of structural units of BO_3 and BO_4 on Sb_2O_4 concentrations. It supports the formation of Sb^{+5} ions and confirms that antimony ions Sb^{+5} play the role of charge compensation of $(BO_4)^-$ and act as a modifier. This result is confirmed with the increase of BO_4 tetrahedral units and non-bridging oxygen. Therefore, the increase of BO_4 units and the non-bridging oxygen enhancement the nonlinear optical properties. The change of density, molar volume, oxygen molar volume, oxygen backing density and N_4 ratio agrees with the FTIR data and reflect the ability of Sb_2O_4 to act as modifier oxide. The observed data clearly suggests that the investigated glasses may be used for optical limiting applications.

Acknowledgement

One of the authors (A. H. Ghanem) would like to thank Prof. M. M. El Okr (Department of Physics, Faculty Science, Al Azhar University, Nasr City, Cairo, Egypt) for his support for choosing this compound and for supporting to carry out this work. (Rahemaho Allah).

References

1. Shelby, J.E., "Introduction to Glass Science and Technology", The Royal Society of Chemistry, UK, 1997.
2. Varshneya, A., "Fundamentals of Inorganic Glasses", Academic Press Inc., New York, 1994.
3. Yano, T., Kunimine, N., Shibata, S., Yamane, M., *J. Non-Cryst. Solids* 321, 137(2003).
4. Stone, C.E., Wright, A.C., Sinclair, R.N., Feller, S., Affatigato, M., Hogan, D.L., Nelson, N.D., Vira, C., Dimitriev, Y.B., Gattef, E.M., Ehrt, D., *Phys. Chem. Glasses* 41(6), 409 (2000).
5. Stehle, C., Vira, C., Hogan, D., Feller, S., Affatigato, M., *Phys. Chem. Glasses* **39** (2), 83 (1998).
6. Zachariasen, W.H., *J. Am. Chem. Soc.* **54**, 3841 (1932).
7. Golunski, S.E. and Jackson, D., *Appl. Catal.* **48**, 123-135 (1989).
8. Golunski, S.E., Nevell, T.G. and Pope, M.I., *Thermochim*, *Acta* **51,** 153-168 (1981).
9. Dumbough, W.H., *Phys. Chem. Glasses* **19**, 121 (1978).
10. Winter, A., J. Am. Ceram. Soc. 40 (1957) 54; A. Winter, *Verres Rebeat* **36**, 35 (1982).
11. Dumbaugh, W. H. and Lapp, J. C., *J. Am. Ceram. Soc.* **75**, 2315 (1992).
12. Hall, D.W., Newhouse, M. A., Borrelli, N.F., Dumbaugh, W.H. and Weidman, D.L., Appl. Phys. Lett.54, 1293 (1989).
13. Vogel, E.M., Weber, M.J., Krol, D.M., *Phys. Chem. Glasses* **32**, 231 (1991).
14. ElBatal, F.H., Azooz, M.A. and Ezz El-Din, F.M., *Phys. Chem. Glasses* **43**, 260 (2002).
15. Rajyasree, Ch., Krishna Rao, D., *J Non-Cryst Solid* **357**, 836–41 (2011).
16. Insiripong, S., Chimalawong, P., Kaewkhao, J., Limsuawan, P., *American J App. Sci.* **8** (6),574–578 (2011).
17. Bhatia, B., Parihar, V., Singh, S., Verma A.S., *Am. J. Condens Matter Phys* **3** (3),80–88 (2013).
18. Kaur, S., Singh, GP., Kaur, P., Singh, DP., *J. Lumin* **143**, 1–37 (2013b).
19. Prajna Shree, M., Wagh, A., Raviprakash, Y., Sangeetha, B., Kamath, SD., *Eur. Sci. J.* **9** (18), 83–92 (2013).
20. SrinivasaRao, CH., Rao, MC., Srikumar, T., *Int. J. Adv. Pharm Biol. Chem.* **2** (3), 549–553 (2013).
21. Eraiah, B., *Bull. Mater.Sci.* **29**, 375–378 (2006).
22. Çelikbilek, M., Ersundu, A.E., Aydin, S., *J. Non-Cryst. Solids* **378**, 247-253 (2013).
23. Ersundu, A.E., Çelikbilek, M., Solak, N., Aydin, S., *J. Eur. Ceram. Soc.* **31**, 2775-2781 (2011).

24. Manal Abdel-Baki, Foud El-Diasty, *J. Solid State Chem.***184**, 2762 (2011).

25. Davis, E.A., Mott, N.F., *Phil. Mag.* **22**, 903 (1970).

26. Chakradhar, R. P. S., Ramesh, K. P., Rao, J. L. and Ramakrishna, J., *J. of Phys. & Chem.* Sol., **64**, 641 (2003).

27. Urbach, J., Phys. Rev. 92, 1324 (1953), doi.: 10.1103/*Phys. Rev.* **92**, 1324 (1953).

28. Singh, D. P., Singh, G. P., *J. Alloy. Compd.* **546**, 224–228 (2013).

29. Masuda, H., Ohta, Y. and Morinaga, K., *J. Jpn. I. Met.***59**, 31 (1995).

30. Orosel, D., Balog, P., Liu, H., Qian, J. and Jansen, M., J. Solid State Chem. 178, 2602 (2005).

31. Som, T., Karmakar, B., *J. Non-Cryst. Solids,* **356**, 987–999 (2010).

32. Terashima, K., Hashimoto, T., Uchnio, Kim, T. S. and Yoko, T., *Journal of the Ceramic Society of Japan* **104**, 1008-1014 (1996).

33. Nalin, M., Messaddeq, Y., Ribeiro, S. J. L., Poulain, M., Briois, V., Brunlkaus, G., Rosenhahn, C., Mosel, B. D. and Eckert, H., *Journal of Materials Chemistry* **14**, 3398-3405 (2004).

34. Galeener, F. L., Lucovsky, G., Mikkelsen, J. C. Jr., *Phys. Rev.* **B 22**, 3983 (1980).

35. Gangareddy Jagannath, Bheemaiah Eraiah, Anuraag Gaddam, Hugo Fernandes, Daniela Brazete, K. Jayanthi, Katturi Naga Krishnakanth, Soma Venugopal Rao, Jose M. F. Ferreira, Annapurna, K. and Amarnath R. Allu, *J. Phys. Chem.* C 123, 5591–5602 (2019).

36. Almeida, A. F. L., Thomazini, D., Vasconelos, I. F., Valente, M. A. and Sombra, A. S. B., *International Journal of Inorganic Materials,* **3**, 829–838 (2001).

37. Kamitsos, E. I., Patsis, A. P., Karakassides, M. A., Chryssikos, G. D., *J. Non-Cryst. Solids* **126**, 52 (1990).

38. Kamitsos, E. I., *Phys. Chem. Glasses* **10**, 79 (2003).

39. Condrat, R., *Introduction to Glass Science* p. 101, (1972).

40. Tarte, P., *Phys. Non-Cryst. Solids* P. 549 (1964).

41. Dimitriev, V., Dimitrov, M., Arnadov, A. C., Topalov, D., *J. Non-Cryst. Solids* **57**, 147 (1983).

42. Jansen, M., *Acta Crystallogr.* **B 35,** 539 (1979).

43. Holland, D., Hannon, A. C., Smith, M. E., Johnson, C. E., Thomas, M. F., Beesley, A. M., Solid State Nucl. Magn. Reson. 26, 172–179 (2004).

44. Doweidar, H., El-Egili, K., Ramadan, R., Al-Zaibani, M., *J. Non-Cryst. Solids* **466**, 37–44 (2017).

45. Flower, G. L., Baskaran, G. S., Reddy, M. S., Veeraiah, N., *Phys.* B **393**, 61–72 (2007).

46. Reddy, M. S., Krishna, G. M., Veeraiah, N., *J. Phys. Chem. Solids* **67**, 789–795 (2006).

47. Abouhaswa, A. S., Mhareb, M. H. A., Amani Alalawi, Al-Buriahi, M. S., *J. Non-Crystalline Solids* **543**, 120130 (2020)

48. Narayana Reddy, C., Sreekanth Chakradhar, R. P., Mater. Res. Bull. 42, 1337 (2007).

49. Doweidar, H., *J. Non-Crystalline Solids* **429**, 112–117 (2015).

50. Parminder Kaur, Singh, K. J., Sonika Thakur, Murat Kurudirek, Mustafa Mohammead Rafiei, *J. Phys. & Chem. Solids,* **150**, 109812 (2021).

51. Doweidar, H., El-Egili, K., Ramadan, R., Al-Zaibani, M., J. *Non-Cryst. Solids* **497**, 93-101 (2018).

52. Rao, M. V., Kumar, V. V. R. K., Shihab, N., Rao, D. N., *Opt. Mater.* **84**, 178–183 (2018).

53. Rao, M. V., Kumar, V. V. R. K., Shihab, N. K., Rao, D. N., *Opt. Laser Technol.* **107**, 110–115 (2018).

دراسة تأثير اضافة Sb_2O_4 على الخواص الفيزيائية والضوئية والبنية التركيبية لزجاج $ZnO\text{-}Na_2O\text{-}B_2O_3$

لقد تم في هذا البحث تحضير عينات من زجاج البورون المطعم بالانتيمون من النوع $10ZnO-25Na_2O-xSb_2O_4$ $(65-x)\ B_2O_3-$ حيث x= 0, 5, 10, 15, 20 mol%. وقد تم بطريقة الانصهار والمسح المتعارف عليها لدراسة الخواص الفيزيائية والضوئية وكذلك البنية التركيبية له. وقد تمت الدراسة باستخدام حيود الاشعة السينية وطيف الامتصاص للاشعة فوق البنفسيجية وكذلك بأستخدام التأثير الطيفي للاشعة تحت الحمراء (XRD, UV visible, FTIR spectroscopy)، حيث اوضحت حيود الاشعة السينية عدم وجود تناسق بلوري للمركب مما يدل على انه ذا طبيعة زجاجية (non-crystalline nature). كما اثبت التأثير الطيفي للاشعة تحت الحمراء FTIR ان Sb_2O_4 يدخل في تركيبة زجاج البورون المطعم باكسيد الزنك والصوديوم كمعدل للبنية التركيبية للزجاج، حيث ان ايون Sb^{+5} يكون كمعوض شحنى لتكوين BO_4 وزيادة القنطرة الغير اكسجينية (non-bridging oxygen)وذلك عن طريق كسر الرابطة Sb-O. وهذا يتسبب في زيادة الكثافة ونقصان كل من طافة الفجوة والنسبة N_4. ان هذا يؤدي الى تغيير الخواص الفيزيائية والضوئية مما يجعلنا نعتقد ان هذا النوع من زجاجات البورون المطعم باكسيد الانتيمون يمكن ان يستخدم في التطبيقات الضوئية.